VIP Drug Delivery Very Important Paper

Deutsche Ausgabe: DOI: 10.1002/ange.201602453
Internationale Ausgabe: DOI: 10.1002/anie.201602453

Magnetically and Near-Infrared Light-Powered Supramolecular Nanotransporters for the Remote Control of Enzymatic Reactions

*Svetlana A. Chechetka, Eiji Yuba, Kenji Kono, Masako Yudasaka, Alberto Bianco, and Eijiro Miyako**

Abstract: *Cancer is one of the primary causes of death worldwide. A high-precision analysis of biomolecular behaviors in cancer cells at the single-cell level and more effective cancer therapies are urgently required. Here, we describe the development of a magnetically- and near infrared light-triggered optical control method, based on nanorobotics, for the analyses of cellular functions. A new type of nanotransporters, composed of magnetic iron nanoparticles, carbon nanohorns, and liposomes, was synthesized for the spatiotemporal control of cellular functions in cells and mice. Our technology will help to create a new state-of-the-art tool for the comprehensive analysis of "real" biological molecular information at the single-cell level, and it may also help in the development of innovative cancer therapies.*

Cancer development starts from one single cell that changes its normal behavior and fate.[1] This transformation from normal to tumor cell is a multistage process, typically representing a progression from a pre-cancerous lesion to malignant tumor. These changes are the result of the interactions between individual genetic factors and external agents. Over the last decades, the analyses of cancer risk factors and the early detection strategies have been developing rapidly.[2] However, a high-precision analysis of the biomolecular behaviors of cancer cells at the single-cell level has not been investigated thoroughly, and efficient therapies are not available yet. Additionally, data demonstrating how anticancer drugs affect a single cancer cell have not been explored. The information about tumor microenvironment, and the development of the strategies for cancer prevention and management could be valuable in a variety of cancer treatments. We believe that many types of cancer can be reduced and controlled by implementing strategies for single-cell manipulation and external control or by a strict control of molecular behaviors in cancer cells.

The emerging field of nanorobotics[3] has the objective to associate different classes of molecules with a variety of materials, in order to obtain new functionalities. This approach also allows the development of advanced and performing devices endowed of multifunctional modalities in different fields of applications, including biomedicine and nanomedicine. In the past decades, the continuous development of nanotechnology has brought innovations in biomedicine, leading to remarkable improvements in the fields of therapy, imaging, and diagnosis.[4–6] The controlled delivery of bioactive agents and the local treatment of diseases represent a novel perspective in the development of efficient multifunctional therapeutics.[7] The future goals of nanorobotics in the fields of biology and biomedicine are those allowing progress in the temporal and spatial site-specific drug delivery, local therapy, imaging, and cellular manipulation of biological processes. However, these studies are still relatively immature. Previously developed nanocomplexes, such as self-assembled and supramolecular nanorobots,[8] DNA nanomachines,[9] and self-powered metal-alloy microrobots,[10–12] have not been thoroughly investigated in vivo. Additionally, more sophisticated manipulations, such as a better directional control of movements and the simplification of controlled drug release at the target sites, are required to achieve the future goals in this field.

The design of advanced nanorobots is another key element in the development of new light technologies for cellular manipulation, which can be exploited in different fields, including caged compounds,[13] optochemical genetics[14] and optogenetics.[15] Ultraviolet,[16] short-wavelength visible,[17] or infrared[18] light has been applied in various optical techniques to control cellular functions. However, light at these wavelengths shows poor penetration into deep biological tissues. Biological systems are instead relatively transparent to light within the diagnostic window between 650 and 1500 nm, except to water absorbance wavelength at 1480 nm.[19] Recently, we synthesized several nanorobots[20–23] that allowed the use of near-infrared (NIR) light (wavelengths 700–2500 nm) that can penetrate into deep tissues. NIR-driven nanorobots have a potential of becoming an ultimate light technology for in vitro and in vivo single-cell manipulations. The high-accuracy control of nanorobot performance in a physiological environment is the next key step for improved cellular manipulations of living organisms.

In this study, we developed a new type of supramolecular nanotransporters based on magnetic iron nanoparticles

[*] Dr. S. A. Chechetka, Dr. M. Yudasaka, Dr. E. Miyako
Nanomaterial Research Institute (NMRI)
National Institute of Advanced Industrial Science and Technology, Central 5, 1-1-1 Higashi
Tsukuba 305-8565 (Japan)
E-mail: e-miyako@aist.go.jp
Dr. E. Yuba, Prof. K. Kono
Department of Applied Chemistry
Graduate School of Engineering
Osaka Prefecture University
1-1 Gakuen-cho, Naka-ku, Sakai, Osaka 599-8531 (Japan)
Dr. A. Bianco
CNRS, Institut de Biologie Moléculaire et Cellulaire, Laboratoire d'Immunopathologie et Chimie Thérapeutique
15 Rue René Descartes, 67084 Strasbourg (France)

Supporting information for this article can be found under: http://dx.doi.org/10.1002/anie.201602453.

(MAG), carbon nanohorns (CNHs), and liposomes with high biocompatibility. These molecular hybrids can easily penetrate into cells by a simple application of magnetic field. Magnetic field- and NIR laser-induced nanotransporters can facilitate the controlled release of substrates from the structures at a target site in cells and organisms, and enable enzymatic reactions. This work represents a proof-of-principle study demonstrating that in vitro and in vivo enzymatic reactions can be mediated by the different functions of the artificial nanorobots, such as those stemming from their magnetic and photothermal properties, leading to the controlled release of loaded molecules. These molecular complexes will provide new opportunities to analyze molecular events in living cells and organisms, to perform comprehensive analyses of the biomolecular processes and provide powerful and multifunctional cancer treatments.

To enable an effective molecular transporter functionality in physiological environment, we used avidin–biotin interactions and self-assembly techniques to synthesize MAG-, oxidized CNH (CNH_{ox})-, and liposome- ($MAG\text{-}CNH_{ox}$-liposome)-based supramolecular hybrids (Figure 1). To prepare these hybrids, avidin-biotin-polyethylenimine (PEI)-MAG-functionalized-CNH_{ox} (avidin-biotin-PEI-MAG-CNH_{ox}) complexes were allowed to spontaneously interact with functionalized liposomes made of 1,2-distearoyl-*sn*-glycero-3-phosphoethanolamine-*N*-[biotinyl(polyethylene glycol)-2000] (biotin-PEG_{2000}-PL) and 1,2-dioleoyl-*sn*-glycero-3-phosphoethanolamine-*N*-(7-nitro-2-1,3-benzoxadiazol-4-yl) (NBD-PE) molecules. NBD molecules on the liposomes were useful for the detection of the supramolecular structure of $MAG\text{-}CNH_{ox}$-liposome nanotransporters by fluorescent microscopy. Green fluorescent particles were observed when $MAG\text{-}CNH_{ox}$ and liposome were mixed in all tested ratios (Figure 2a and Figure S1 in the Supporting Information). We did not detect the strong fluorescence signal of separated avidin-biotin-PEI-MAG-CNH_{ox} and functional liposomes (liposome:avidin-biotin-PEI-MAG-CNH_{ox} ratio = 1:0 and 0:100). The fluorescent particle size was the smallest when the ratio of liposome:avidin-biotin-PEI-MAG-CNH_{ox} was 1:100. Larger aggregates were formed at the other analyzed ratios (liposome:avidin-biotin-PEI-MAG-CNH_{ox} = 1:25, 1:50, 1:75). These results indicate that the optimal combination between the functional liposome and avidin-biotin-PEI-MAG-CNH_{ox} is 1:100, which we used in the next experiments, including dynamic light scattering (DLS; Table S1). When this ratio was investigated, we observed "teddy bear"-shaped supramolecular $MAG\text{-}CNH_{ox}$-liposome assemblies using transmission electron microscopy (TEM; Figures 2b and S2). TEM showed that CNHs (average diameter ca. 50 nm, $n = 100$) decorated the surface of the liposomes (average diameter ca. 150 nm, $n = 100$), as shown in Figure 1a. The average number of CNHs on the molecular complexes was about 2.3. These results reveal that the synthesized $MAG\text{-}CNH_{ox}$-liposome nanotransporters have supramolecular structures stabilized by avidin-biotin interactions.

Next, we investigated the cytotoxicity of $MAG\text{-}CNH_{ox}$-liposome nanotransporters, as this is a very important issue not only for the control of enzymatic reactions in physiological conditions but also for future biomedical applications.

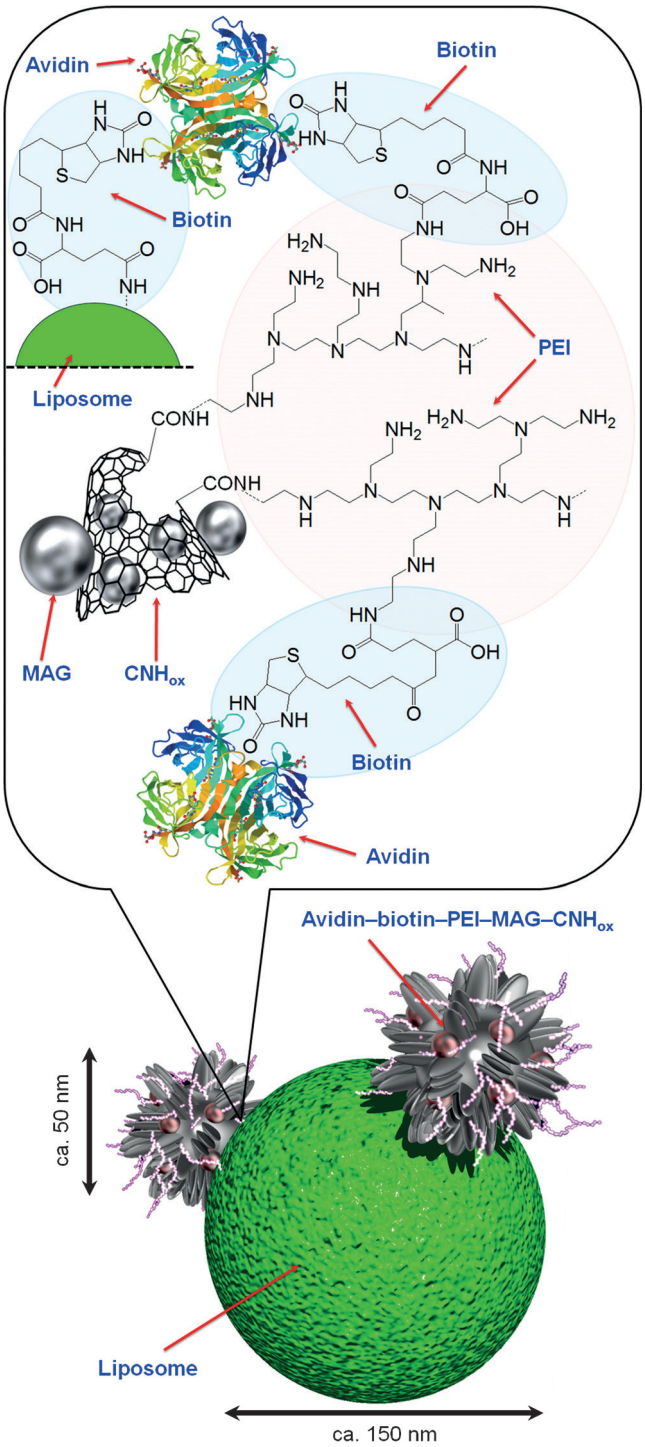

Figure 1. Schematic illustration of the nanotransporters.

The survival of human cervical cancer cells (HeLa) was investigated using WST-1 assays (Figure 2c). HeLa cells were pre-incubated with three different concentrations (CNH = 5, 10, or 25 $\mu g\,mL^{-1}$, lipids in liposome = 3, 6, or 15 μM, respectively). We showed that over 90% cells were viable following the treatment, likely thanks to the water-dispersing properties and the high biocompatibility of PEG[24] at the interfaces of the liposomes. Previously, we confirmed, through

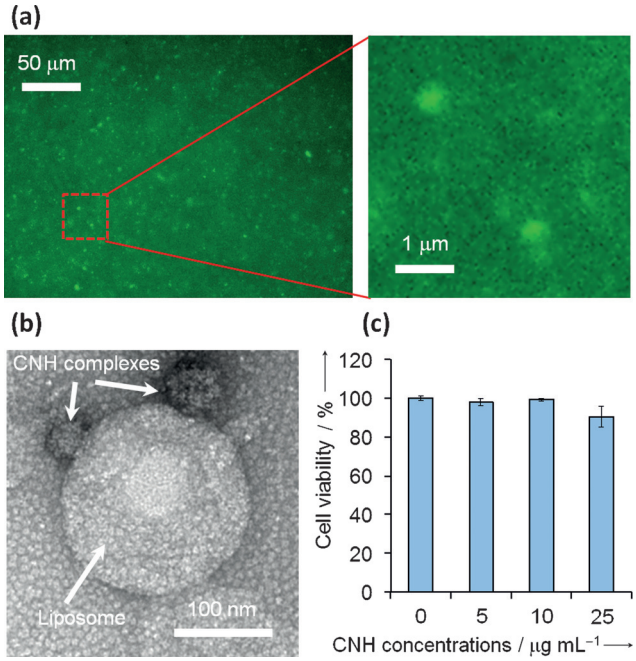

Figure 2. Characterization of MAG-CNH_{ox}-liposome supramolecular nanotransporters. a) Fluorescence micrographs of nanotransporters (CNH = 167 μg mL^{-1}, lipid in liposomes = 25 μM). b) TEM image of the nanotransporter structure. Sample concentration used: CNH = 10 μg mL^{-1}, lipids in the liposomes = 6 μM. c) WST-1 HeLa cell assays after 24 h incubation with the nanotransporters (CNH = 0, 5, 10, and 25 μg mL^{-1}, lipid in liposomes = 0, 3, 6, and 15 μM). Data represent the mean of three measurements; error bars show the SD.

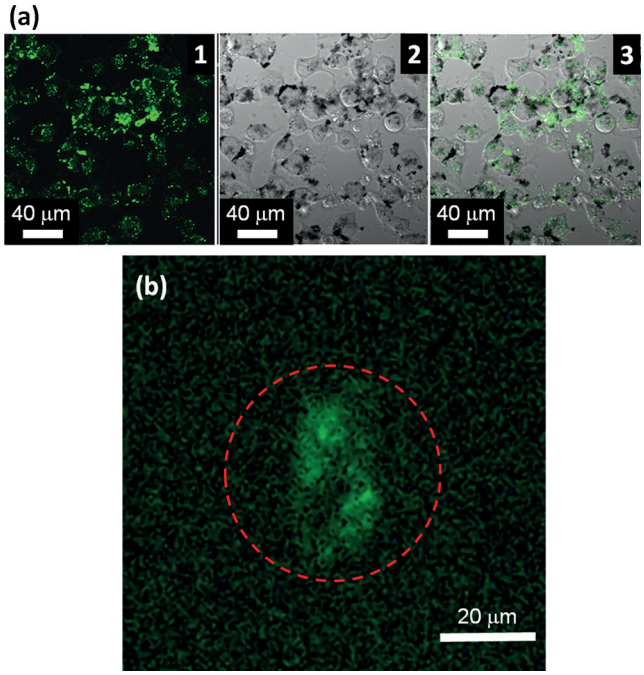

Figure 3. In vitro remote control of enzymatic reactions using nanotransporters. a) Confocal microscope images (λ_{ex} = 488 nm, λ_{em} = 510 nm) of HeLa cells after incubation with fluorescent NBD-labeled MAG-CNH_{ox}-liposome for 4 h with a magnet (CNH = 10 μg mL^{-1}, lipid in the liposomes = 6 μM). Fluorescence (1), differential interference contrast (DIC; 2), and combination of fluorescence and DIC images (3). b) Remote control of β-Gal reactions in the target cells by laser-induced nanotransporters encapsulating FDG (CNH = 10 μg mL^{-1}, lipid in liposome = 6 μM, and FDG = 6.7 nM). Magnification: 20×. Laser power: 301 mW (153 μW μm^{-2}). The red dashed circle shows the irradiated cites.

several in vitro[21,25] and in vivo[21,26,27] assays, that CNHs were non-toxic.

Direct transport of the vectors to the target sites is one of the primary goals of molecular transport technology and drug delivery. Magnetic field is generally used to attract nanomaterials that have magnetic characteristics.[28,29] Therefore, we studied the internalization and distribution of nanotransporters into the HeLa cells, using the magnetic field-induced MAG-CNH_{ox}-liposomes (CNH = 10 μg mL^{-1}, lipid concentration in liposomes = 6 μM; Figures 3 a, S3, and S4). HeLa cells were incubated with the nanotransporters for 4 h, with or without a magnet. The intracellular uptake of the nanotransporters was assessed using laser confocal microscopy. Green fluorescence emission and black aggregates of the nanotransporters were observed at the intracellular and extracellular levels. Notably, MAG-CNH_{ox}-liposomes more effectively accumulated into the cells when the magnetic field was applied using a neodymium magnet (450 mT), due to the strong ferromagnetic properties of MAG-CNH_{ox} complexes (saturation magnetization was 49 ± 1 emu g^{-1} at 300 K).[30,31] Additionally, these nanotransporters displayed a higher level of spontaneous cellular uptake, compared with the NBD-labeled liposomes alone, without the application of a magnetic field, as observed by an increased intensity of fluorescence into the cells incubated with the different nanohybrids (Figure S3). Furthermore, MAG-CNH_{ox}-liposomes were insignificantly cytotoxic (cell viability was over 80 %) after the application of the magnetic field for 24 h (Figure S5). These results indicate that the interactions of magnetic field-induced nanotransporters with the cells are effective and safe.

During the development of the system for in vitro and in vivo remote control of enzymatic reactions, we employed the model reaction involving β-galactosidase (β-Gal), which is mainly overexpressed in primary ovarian, breast, and colorectal cancers,[32] using two types of cell lines (i.e. mouse GP8 cells overexpressing human β-Gal as a positive control, and SV40 immortalized β-Gal gene deficient mouse fibroblasts as a negative control). Non-fluorescent fluorescein di-β-D-galactopyranoside (FDG) was encapsulated inside liposomes, made only of biotin-PEG_{2000}-PL and PE, to directly observe β-Gal enzymatic reaction in cells. As the photothermal properties of CNHs lead to the destruction of liposomes, FDG is then released from the hybrids, it is hydrolyzed by intracellular β-Gal to fluorescein as a strong green fluorescent moiety, and the resulting fluorescence emission can be monitored. We previously demonstrated that liposome structures can be effectively destroyed at a temperature above 42 °C by adjusting the chemical composition and manipulating the photothermal properties of the carbon nanotubes.[20,23] Here, bright green-colored fluorescence emission triggered by β-Gal enzymatic reaction was observed immediately (within 0.03 s) in a single target GP8 cell upon irradiation with a NIR laser (808 nm), and after the application of the

magnetic field for 4 h [Figures 3b and see Supporting Movie, M1]. The observation of the change in florescence was limited to a single cell due to the use of highly focused laser beam (laser spot diameter = 50 μm). Additionally, the fluorescence emission generated by the β-Gal reaction was monitored when the applied laser power values ranged from 204–301 mW (104–153 $\mu W\,\mu m^{-2}$). The structure and size of GP8 cells did not change when the highest laser power (301 mW, 153 $\mu W\,\mu m^{-2}$) was applied, although the result was that the cells died. Indeed, we observed the appearance of bubbles when the applied power was more than 301 mW (Figure S6 and see Supporting Information for a movie, M2). Therefore, we believe that the optimal laser power should be less than 301 mW for further in vitro experiments. In the control experiments, without the application of the magnetic field, we did not observe any fluorescence emissions (Figure S7b). The FDG-encapsulated liposomes and avidin-biotin-PEI-MAG-CNH_{ox} alone did not emit fluorescence in the GP8 cell line, even after the application of the magnetic field (Figure S7c and S7d). In the experiments using negative control SV40 immortalized β-Gal gene deficient mouse fibroblasts, the fluorescence emission was not observed when our nanotransporters were used (Figure S7e). These results demonstrate that β-Gal enzyme activity in the targeted cells can be remotely controlled using our magnetic field- and laser-induced nanotransporters.

Blood vessels are involved in many biological processes, such as the transport of biomolecules, the maintenance of homeostasis, and the development of cancer metastases.[33] Succeeding in the manipulation of biomolecular information in blood vessels using nanotransporters would represent a milestone for nanorobotics, and it could be additionally exploited for the development of effective cancer treatments. Therefore, we monitored the accumulation of the magnetic field-induced nanotransporters in the blood vessels of mice. Various nanomaterial suspensions (MAG-CNH_{ox}-liposomes, NBD-labeled liposomes, avidin-biotin-PEI-MAG-CNH_{ox}, and MES buffer) were injected into the caudal vein of mice, and the experiments were performed with or without the application of a magnetic field, with the magnet placed on mouse ears, to attract the nanotransporters (Figure 4a). We selected the ears to monitor the physicochemical behavior of the nanotransporters in blood vessels because it is a relatively thin organ, representing a convenient place for microscopic observations.[34] Bright green-colored fluorescence in the blood vessels, originating from NBD-labeled nanotransporters, was measured following the application of the magnetic field to the animal ears (Figures 4b and S8a). The nanotransporters, without the application of the magnetic field, showed slight fluorescence emission in the blood vessels of the ear, much weaker than the florescence measured in the presence of the magnetic field-induced samples (Figure S8b). Little fluorescence was instead observed in the other control experiments (NBD-labeled liposomes, avidin-biotin-PEI-MAG-CNH_{ox}, and MES buffer without nanotransporters) regardless of the presence or the absence of the magnetic field (Figures S8c–h). These results demonstrate that magnetic field-induced nanotransporters can effectively accumulate at the target sites by a simple application of an external magnet.

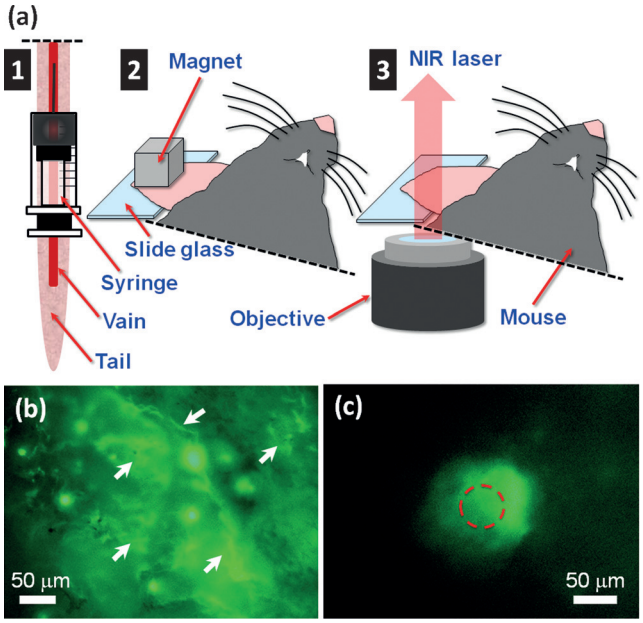

Figure 4. In vivo remote control of enzymatic reactions using nanotransporters. a) Schematic illustration of the experimental setups (1: Intravenous injection of nanotransporters from a tail vein of a mouse, 2: Accumulation of nanotransporters by a neodymium magnet, 3: Observation and manipulation of physicochemical properties of nanotransporters with NIR laser irradiation). b) Magnetic field-induced accumulation of nanotransporters in blood vessels of a mouse ear. White arrows show the accumulated nanotransporters in blood vessels. c) The direct observation of in vivo β-Gal reaction in living mouse triggered by magnetic field- and laser-induced nanotransporters encapsulating FDG (CNH = 100 $\mu g\,mL^{-1}$, lipid in liposomes = 60 μM, and FDG = 67 nM). Magnification: 20×. Laser power: 301 mW (153 $\mu W\,\mu m^{-2}$). The red dashed circle indicates the irradiated sites.

Finally, in vivo remote control of the enzymatic reaction was monitored using transgenic CG mice overexpressing human β-Gal in the whole body (Figures 4c, S9, and S10). Bright green fluorescence, originating from the magnetic field- and laser-driven nanotransporters that enable β-Gal enzymatic reaction, was observed in the blood vessels of the ear of transgenic mice (Figures 4c, S9a and see Supporting Movie, M3). In the control experiment, using laser-induced nanotransporters without the application of the magnet, fluorescence was completely absent (Figure S9b). Additionally, fluorescence was not observed in other control experiments (liposome encapsulating FDG, avidin-biotin-PEI-MAG-CNH_{ox}, and MES buffer; Figure S9c–h). We were not able to observe green fluorescence in wild-type mice using all types of nanomaterials, including nanotransporters encapsulating FDG, regardless of the presence of a magnetic field and the laser induction (Figure S10). Therefore, we believe that the magnetic field- and laser-induced nanotransporters encapsulating FDG are able to mediate β-Gal enzymatic reaction in β-Gal-rich transgenic mice. Furthermore, nanomaterial injections did not affect the viability and body weight of mice up to 30 days (Figure S11). These results indicate that our highly biocompatible nanotransporters function efficiently in the living organisms as magnetic field- and laser-induced supramolecular nanorobots.

In summary, magnetic field- and laser-induced highly performant nanorobots, based on MAGs, CNHs, and liposomes, were successfully developed through a simple self-assembly strategy. We succeeded in synthesizing supramolecular hybrids with high biocompatibility, strong magnetic characteristics and effective photothermal properties, enabling spatiotemporal controlled release of substrates from the structures at the desired location in cells and mouse bodies, using a magnet and a NIR laser in a non-contact manner. To the best of our knowledge, this represents the first demonstration of remotely controlled enzymatic reactions that relies on the application of a strong magnetic field, and powerful photothermal and substrate-controlled-release properties of combined materials. Artificial nanorobots represent a promising technology for uses in materials science and biomedicine. Especially, the use of the nanorobots would be beneficial for remote control of a wide range of enzymatic biomakers such as glutathione transferases[35] and γ-glutamyltranspeptidase[36] in microenvironment of cancer cells. In addition, the application of this technology utilizing biological tissue-penetrating NIR lasers may be advantageous for the innovative molecular transport systems, such as active targeting and delivery of drugs and advanced optochemical genetics.

Acknowledgements

This work was supported by a Japan Society for the Promotion of Science (JSPS) KAKENHI Grant-in-Aid for Scientific Research (B) (grant number 16H03834), a JSPS KAKENHI Grant-in-Aid for Young Scientists (A; grant number 25702030), a JSPS KAKENHI Grant-in-Aid for Challenging Exploratory Research (grant numbers 15K13309 and 16K13632), the Foundation Advanced Technology Institute, the Centre National de la Recherche Scientifique (CNRS), the Agence Nationale de la Recherche (ANR) through the LabEx project Chemistry of Complex Systems (grant number ANR-10-LABX-0026 CSC), and by the International Center for Frontier Research in Chemistry (icFRC). A.B. thanks to JSPS for the Invitation Fellowship in Japan (long-term grant L-15526). We thank Ms. Emiko Kobayashi (Bioproduction Research Institute, AIST) and ICT, Biotechnology, Energy & Environment Tech., Converging Tech. (IBEC) for providing an innovative platform for TEM observations.

Keywords: carbon nanohorns · drug delivery systems · liposomes · magnetic nanoparticles · nanorobots

How to cite: *Angew. Chem. Int. Ed.* **2016**, *55*, 6476–6481
Angew. Chem. **2016**, *128*, 6586–6591

[1] R. A. Weinberg, *The Biology of Cancer*, 2nd ed., Garland, New York, **2013**.
[2] M. H. Hamdan, D. M. Desiderio, N. M. Nibbering, *Cancer Biomarkers: Analytical Techniques for Discovery*, Wiley-VCH, Weinheim, **2007**.
[3] K. E. Drexler, M. Minsky, *Engines of Creation: The Coming Era of Nanotechnology*, Anchor Press, Doubleday, **1986**.
[4] C. A. Mirkin, C. M. Niemeyer, *Nanobiotechnology II,: More Concepts and Applications*, Wiley-VCH, Weinheim, **2007**.
[5] C. Ménard-Moyon, H. Ali-Boucetta, C. Fabbro, O. Chaloin, K. Kostarelos, A. Bianco, *Chem. Eur. J.* **2015**, *21*, 14886–14892.
[6] L. G. Delogu, G. Vidili, E. Venturelli, C. Ménard-Moyon, M. A. Zoroddu, G. Pilo, P. Nicolussi, C. Ligios, D. Bedognetti, F. Sgarrella, R. Manetti, A. Bianco, *Proc. Natl. Acad. Sci. USA* **2012**, *109*, 16612–16617.
[7] S. Svenson, R. K. PruO'homme, *Multifunctional Nanoparticles for Drug Delivery Applications: Imaging, Targeting, and Delivery*, Springer, New York **2012**.
[8] G. M. Whitesides, J. P. Mathias, C. Seto, *Science* **1991**, *254*, 1312–1319.
[9] B. Yurke, A. J. Turberfield, A. P. Mills Jr, F. C. Simmel, J. L. Neumann, *Nature* **2000**, *406*, 605–608.
[10] M. Ibele, T. E. Mallouk, A. Sen, *Angew. Chem. Int. Ed.* **2009**, *48*, 3308–3312; *Angew. Chem.* **2009**, *121*, 3358–3362.
[11] S. Campuzano, J. Orozco, D. Kagan, M. Guix, W. Gao, S. Sattayasamitsathit, J. C. Claussen, A. Merkoçi, J. Wang, *Nano Lett.* **2012**, *12*, 396–401.
[12] S. Sanchez, A. N. Ananth, V. M. Fomin, M. Viehrig, O. G. Schmidt, *J. Am. Chem. Soc.* **2011**, *133*, 14860–14863.
[13] G. Mayer, A. Heckel, *Angew. Chem. Int. Ed.* **2006**, *45*, 4900–4921; *Angew. Chem.* **2006**, *118*, 5020–5042.
[14] T. Fehrentz, M. Schönberger, D. Trauner, *Angew. Chem. Int. Ed.* **2011**, *50*, 12156–12182; *Angew. Chem.* **2011**, *123*, 12362–12390.
[15] Special issue on Optogenetics, (Ed.: M. Baker), *Nat. Methods* **2011**, *8*, 19–42.
[16] H. Ye, M. D. E. Baba, R.-W. Peng, M. Fussenegger, *Science* **2011**, *332*, 1565–1568.
[17] G. Leitz, E. Fällman, S. Tuck, O. Axner, *Biophys. J.* **2002**, *82*, 2224–2231.
[18] M. G. Shapiro, K. Homma, S. Villarreal, C.-P. Richter, F. Bezanilla, *Nat. Commun.* **2012**, *3*, 736.
[19] R. Weissleder, *Nat. Biotechnol.* **2001**, *19*, 316–317.
[20] E. Miyako, K. Kono, E. Yuba, C. Hosokawa, H. Nagai, Y. Hagihara, *Nat. Commun.* **2012**, *3*, 1226.
[21] E. Miyako, T. Deguchi, Y. Nakajima, M. Yudasaka, Y. Hagihara, M. Horie, M. Shichiri, Y. Higuchi, F. Yamashita, M. Hashida, Y. Shigeri, Y. Yoshida, S. Iijima, *Proc. Natl. Acad. Sci. USA* **2012**, *109*, 7523–7528.
[22] E. Miyako, J. Russier, M. Mauro, C. Cebrian, H. Yawo, C. Ménard-Moyon, J. A. Hutchison, M. Yudasaka, S. Iijima, L. De Cola, A. Bianco, *Angew. Chem. Int. Ed.* **2014**, *53*, 13121–13125; *Angew. Chem.* **2014**, *126*, 13337–13341.
[23] E. Miyako, S. A. Chechetka, M. Doi, E. Yuba, K. Kono, *Angew. Chem. Int. Ed.* **2015**, *54*, 9903–9906; *Angew. Chem.* **2015**, *127*, 10041–10044.
[24] F. F. Davis, *Adv. Drug Delivery Rev.* **2002**, *54*, 457–458.
[25] H. Isobe, T. Tanaka, R. Maeda, E. Noiri, N. Solin, M. Yudasaka, S. Iijima, E. Nakamura, *Angew. Chem. Int. Ed.* **2006**, *45*, 6676–6680; *Angew. Chem.* **2006**, *118*, 6828–6832.
[26] Y. Tahara, J. Miyawaki, M. Zhang, M. Yang, I. Waga, S. Iijima, H. Irie, M. Yudasaka, *Nanotechnology* **2011**, *22*, 265106.
[27] J. Miyawaki, M. Yudasaka, T. Azami, Y. Kubo, S. Iijima, *ACS Nano* **2008**, *2*, 213–226.
[28] X. Mou, Z. Ali, S. Li, N. He, *J. Nanosci. Nanotechnol.* **2015**, *15*, 54–62.
[29] E. Miyako, B. P. Pichon, C. Ménard-Moyon, I. A. Vacchi, C. Lefèvre, S. Bégin-Colin, A. Bianco, *Carbon* **2016**, *96*, 49–56.
[30] S. A. Chechetka, B. Pichon, M. Zhang, M. Yudasaka, S. Bégin-Colin, A. Bianco, E. Miyako, *Chem. Asian J.* **2015**, *10*, 160–165.
[31] S. A. Chechetka, M. Zhang, M. Yudasaka, E. Miyako, *Carbon* **2016**, *97*, 45–53.
[32] D. Asanuma, M. Sakabe, M. Kamiya, K. Yamamoto, J. Hiratake, M. Ogawa, N. Kosaka, P. L. Choyke, T. Nagano, H. Kobayashi, Y. Urano, *Nat. Commun.* **2015**, *6*, 6463.

[33] Y. C. Fung, *Biomechanics: Mechanical Properties of Living Tissues*, Springer, New York, **1993**.
[34] M. C. Zhong, X.-B. Wei, J.-H. Zhou, Z.-Q. Wang, Y.-M. Li, *Nat. Commun.* **2013**, *4*, 1768.
[35] J. Zhang, A. Shibata, M. Ito, S. Shuto, Y. Ito, B. Mannervik, H. Abe, R. Morgenstern, *J. Am. Chem. Soc.* **2011**, *133*, 14109.
[36] Y. Urano, M. Sakabe, N. Kosaka, M. Ogawa, M. Mitsunaga, D. Asanuma, M. Kamiya, M. R. Young, T. Nagano, P. L. Choyke, H. Kobayashi, *Sci. Transl. Med.* **2011**, *3*, 110ra119.

Received: March 9, 2016
Published online: April 15, 2016

